

Metastable orbital order in nanoscale LaMnO_3 below a critical size $d_C \sim 20$ nm

Parthasarathi Mondal and Dipten Bhattacharya,^{*}
*Sensor & Actuator Division, Central Glass and Ceramic Research Institute, CSIR,
Kolkata 700032, India*

Dipshikha Bhattacharya[†] and Omprakash Chakrabarti
*Non-Oxide Ceramic and Composite Division, Central Glass and Ceramic Research Institute,
CSIR, Kolkata 700032, India*

We report that the orbital ordered state in nanoscale LaMnO_3 is metastable below a critical size $d_C \sim 20$ nm. The orbital order-disorder transition switches from reversible to irreversible at d_C with 2-4% decay in resistance in the orbital ordered state over a time scale of ~ 3000 s. The orbital disordered phase, in contrast, is quite stable with virtually no decay in resistance with time. The disordered phase with stable resistance could be dragged down to room temperature from above the transition temperature. In a single crystal of LaMnO_3 , both the ordered and disordered phases are stable.

PACS Nos. 71.70.Ej; 75.50.Tt

^{*}Corresponding author; e-mail: dipten@cgcri.res.in

[†]Present address: Department of Chemistry, IIT Kharagpur, Kharagpur 721302, India

The study of phase stability and transition in confined geometry (e.g., in nanoscale system) assumes significance both for its physics as well as for the design of different nanosized architectures to be used in nanoelectronics. Although, this has been addressed, theoretically, more than 30 years back,¹ direct measurement of the phase stability and transition enthalpy together with its kinetics is being reported²⁻⁴ only in recent times. Several novel approaches – such as scanning tunneling microscopy together with perturbed angular correlation,² laser irradiation coupled with local calorimetry,³ ultrasensitive nanocalorimetry⁴ etc – have been adopted for measuring the melting point and latent heat of melting in nanoscale atomic clusters. Deeper understanding of the phase transition thermodynamics and kinetics of electronic phase superstructures⁵ – such as charge and orbital order – is also of immense importance for nanosized strongly correlated electron systems.

In pure LaMnO₃, the orbital order superstructure develops due to degeneracy in 3d e_g levels in Mn³⁺O₆ octahedra which is lifted via Jahn-Teller effect resulting in a cooperative ordering of the $d_{3x^2-r^2}$ and $d_{3y^2-r^2}$ orbitals within the ab-plane and their staggered stacking along the c-axis (so-called ‘d’-type orbital order).⁶ The orbital ordered state undergoes an order-disorder transition at a characteristic transition point T_{IT}.⁷ This is accompanied by a structural transition⁸ as well as characteristic features⁹ in different physical properties such as resistivity, thermoelectric power, Curie-Weiss paramagnetism, specific heat, thermal expansion coefficient etc.

In this paper, we report that the nature of the orbital order-disorder transition switches from ‘irreversible’ to ‘reversible’ in nanoscale LaMnO_3 at a critical size $d_C \sim 20$ nm which signifies that at and below d_C the orbital ordered state is metastable. We have studied the relaxation characteristics of the resistivity both in the ordered and disordered states and found that the resistivity decays with time in the ordered state but not in the disordered state. In contrast, in a single crystal as well as in nanoscale LaMnO_3 of size above d_C , the orbital ordered state is stable and the order-disorder transition is reversible at characteristic T_{JTS} .

The nanoscale particles of phase pure LaMnO_3 system have been prepared via several routes: (i) sonochemical synthesis,¹⁰ (ii) synthesis from microemulsion,¹⁰ and (iii) carbon replica of bio-templates – stems of pine wood – assisted synthesis. The template walls (of pore dia $\sim 10\text{-}40$ μm) appear to contain porous channels with size range 5-10 nm (Fig. 1). In the case of bio-template-assisted synthesis, the mixed metal nitrate solution is infiltrated within such templates under vacuum. Following infiltration, the sample is first dried at 100°C and then heat treated at 700°C for 2h. The remnant after heat treatment is found to be phase pure LaMnO_3 powder (Fig. 2c). It is interesting to note that we observe presence of nanorods (dia $\sim 15\text{-}20$ nm and above) as well as nanochains along with nearly spherical nanoparticles (Fig. 2) only in the case of samples prepared by using the carbon replica of bio-templates. We carried out the electrical resistivity measurements directly on such nanoscale particles by preparing a slurry using LaMnO_3 powder dispersed within an alumina sol. The slurry is, then, coated onto an alumina substrate having gold electrodes and wires printed on it.

The characteristic features in the resistivity versus temperature patterns at respective T_{JTS} could be noticed. The T_{JTS} , thus found out, match closely with the T_{JT} s identified from the peaks in the calorimetric studies¹⁰ for the particles of sizes above d_C for which peaks in the calorimetry measurement appear. For the samples of size d_C and less, no peak in the calorimetric study could be noticed. The resistivity (ρ) versus temperature (T) pattern for a sample of size d_C is shown in Fig. 3a. Close inspection of the pattern, observed at an applied current 50 μ A, shows that there is a clear signature of orbital order-disorder transition at T_{JT} (~630 K). *However, the transition appears to be irreversible.* No signature of disorder-order transition could be noticed during the cooling cycle. Instead, the ρ -T pattern observed at orbital disordered state beyond T_{JT} appears to have been extended right down to ~300 K. A second run, under identical applied current, does not depict any signature of transition at all, at any temperature within 300-800 K. This is quite a new observation, as this has never been observed in the bulk system. For comparison, we show in Fig. 3b the ρ -T patterns (both heating and cooling cycles) for a single crystal of LaMnO₃. The transition is reversible at T_{JT} ~750 K.

In order to gather more information about the stability of the orbital ordered state in samples of size d_C and below, we measured the relaxation characteristics – i.e., time dependence of the resistivity – at below and above T_{JT} following two different protocols: (i) heating a fresh sample to the respective points and then initiating the relaxation measurement after stabilizing the temperature and (ii) heating the sample beyond T_{JT} up to ~800 K and then cooling down to the respective points. The temperatures chosen for the relaxation studies are: (i) ~410 K (i.e., well below T_{JT}), (ii) ~618 K (i.e., near the T_{JT})

and (iii) ~ 765 K (i.e., well above T_{JT}). We repeated the relaxation studies both in the samples of size above d_C and in a single crystal by choosing the temperatures appropriately. The relaxation was measured by reaching and stabilizing the temperature first and then by triggering the current flow and voltage recording simultaneously. The data were recorded at a time interval of ~ 43 ms over a time span of ~ 3000 s. The relaxation characteristics are shown in Figs. 3c,d. Quite evident in Fig. 3c is the fact that as the temperature is increased from well below T_{JT} to close to T_{JT} , the decay rate of the resistivity increases appreciably. However, well above T_{JT} no decay in resistivity could be noticed. Likewise, no decay in resistivity could be noticed when the sample is cooled down to the lower temperatures from above T_{JT} and relaxation measurement is done at those points. This observation further supports the conjecture that the orbital ordered state in samples of size d_C and below is metastable. The decay rate enhances near T_{JT} because of enhanced fluctuations arising from onset of transition dynamics in a metastable phase. The disordered state is quite stable and depicts no appreciable decay in resistivity. The single crystal and the samples of size greater than d_C depict stable ordered and disordered states (Fig. 3d).

The decay patterns of resistivity in samples of size d_C and below appear to be approximately linear with time over the range studied. We have calculated the activation energy (E) of decay by fitting the data with $\frac{R(t)}{R(0)} = c - \frac{k_B T}{E} \cdot (t/\tau)$ equation where c is a constant and τ is a relaxation time scale. The activation energy is found to decrease from ~ 36 meV to ~ 6 meV over a temperature range 411-618 K. The linear relaxation pattern points out that the relaxation process is slow in the shorter time scale and faster than any

other nonlinear processes in the longer time scale. Similar ‘linear in time relaxation pattern’ was observed¹¹ for recovery of magnetization from saturation in the superfluid ³He. The physics behind such linear relaxation for the present case is currently unknown.

It has been shown earlier by others¹²⁻¹³ that the charge-ordered systems undergo a melting type transition in nanoscale because of enhanced pressure effect. In fact, the phenomenon of melting of the charge ordered state under pressure, associated with insulator to metal and antiferromagnetic to ferromagnetic transitions, appears to have been replicated well in the nanoscale system. However, it is to be noted that an ordered structure such as charge or orbital order possesses a fundamental length scale or domain size. The samples of size smaller than the domain size should exhibit fluctuations or metastability. One can draw an analogy here between these systems and the conventional ferromagnets. In a nanoscale sample of size below the size of a single ferromagnetic domain, the ferromagnetic order gives way to fluctuating ‘superparamagnetic’ state above the blocking temperature. Piecing together, it seems that although pressure does increase in the nanoscale sample because of enhanced surface area to volume ratio, the melting from a stable ordered state to a stable disordered state takes place via an intermediate metastable state where the pressure is not sufficient for melting. In fact, in the present case, we did not observe metal-insulator transition or ferromagnetism in nanoscale LaMnO₃ at sizes d_C or below as reported for charge ordered compounds by others.¹²⁻¹³ In the light of the observation made here, it will be interesting to find out the fundamental length scale or domain size of the orbital order in pure LaMnO₃. It is also interesting to note that the symmetry of the crystallographic structure does not change at

or below d_C . This observation shows that the stability of the orbital order phase is not quite strongly related to the underlying crystallographic phase.

In summary, we found that the orbital ordered state in pure LaMnO_3 becomes metastable for particles of size d_C (~ 20 nm) and below. The orbital order-disorder transition switches from ‘reversible’ to ‘irreversible’ at d_C along with sizable decay in resistivity with time in the ordered state. In contrast to the observation made in the case of charge ordered compounds, we did not observe an insulator-metal transition and antiferromagnetic-ferromagnetic transition for a size below d_C . It is interesting to note that this metastable orbital ordered state does not depict any change in the symmetry of the crystallographic structure.

The authors thank P. Choudhury for helpful discussion and N. Das for her association in the initial phase of the work. They also thank P. Mandal (SINP, Kolkata) for providing the single crystal of LaMnO_3 . One of the authors (PM) acknowledges financial support from CSIR while another author (OPC) thanks DST for a sponsored project.

- ¹Ph. Buffat and J.-P. Borel, *Phys. Rev. A* **13**, 2287 (1976).
- ²M. Dippel, A. Maier, V. Gimple, H. Wider, W.E. Evenson, R.L. Rasera, and G. Schatz, *Phys. Rev. Lett.* **87**, 095505 (2001).
- ³M. Zhang, M.Y. Efremov, F. Schiettekatte, E.A. Olson, A.T. Kwan, S.L. Lai, T. Wisleder, J.E. Green, and L.H. Allen, *Phys. Rev. B* **62**, 10548 (2000).
- ⁴M. Schmidt, R. Kusche, B. von Issendorf, and H. Haberland, *Nature (London)* **393**, 238 (1998).
- ⁵See, for example, Y. Tokura and N. Nagaosa, *Science* **280**, 462 (2000).
- ⁶S. Okamoto, S. Ishihara, and S. Maekawa, *Phys. Rev. B* **65**, 144403 (2002).
- ⁷Y. Murakami, J.P. Hill, D. Gibbs, M. Blume, I. Koyama, M. Tanaka, H. Kwata, T. Arima, Y. Tokura, K. Hirota, and Y. Endoh, *Phys. Rev. Lett.* **81**, 582 (1998).
- ⁸J.R. Carvajal, M. Hennion, F. Moussa, A.H. Moudden, L. Pinsard, and A. Revcolevschi, *Phys. Rev. B* **57**, R3189 (1998).
- ⁹See, for example, J.-S. Zhou and J.B. Goodenough, *Phys. Rev. B* **60**, R15002 (1999).
- ¹⁰N.Das, P. Mondal, and D. Bhattacharya, *Phys. Rev. B* **74**, 014410 (2006).
- ¹¹See, for example, L.R. Corruccini and D.D. Osheroff, *Phys. Rev. Lett.* **34**, 564 (1975).
- ¹²T. Sarkar, B. Ghosh, A.K. Raychaudhuri, and T. Chatterji, *Phys. Rev. B* **77**, 235112 (2008).
- ¹³T. Sarkar, A.K. Raychaudhuri, and T. Chatterji, *Appl. Phys. Lett.* **92**, 123104 (2008).

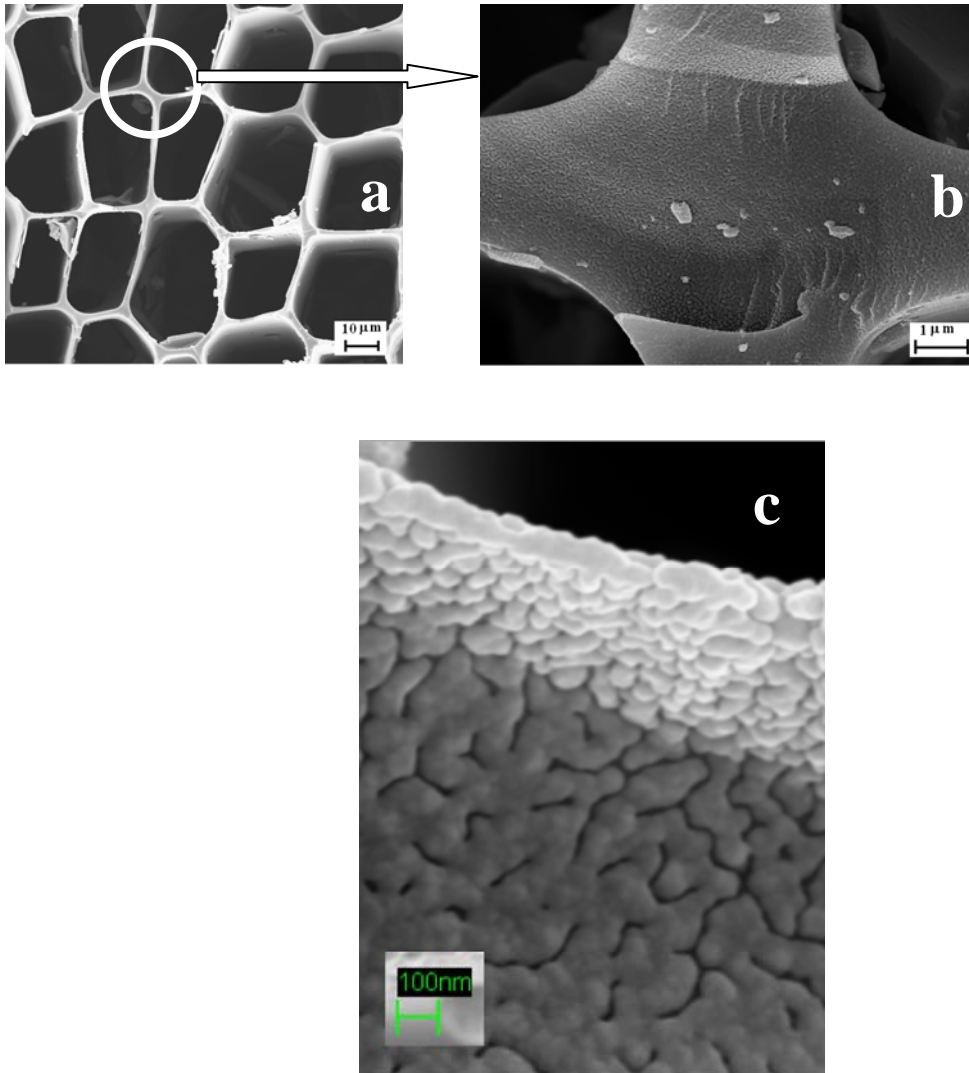


Fig.1. (a) Field effect scanning electron micrograph (FESEM) of the porous carbon replica of bio-template (stem of pine wood), (b) blown up photograph of the wall of the bigger pore channels and (c) the finer pore structure (5-10 nm) of the wall.

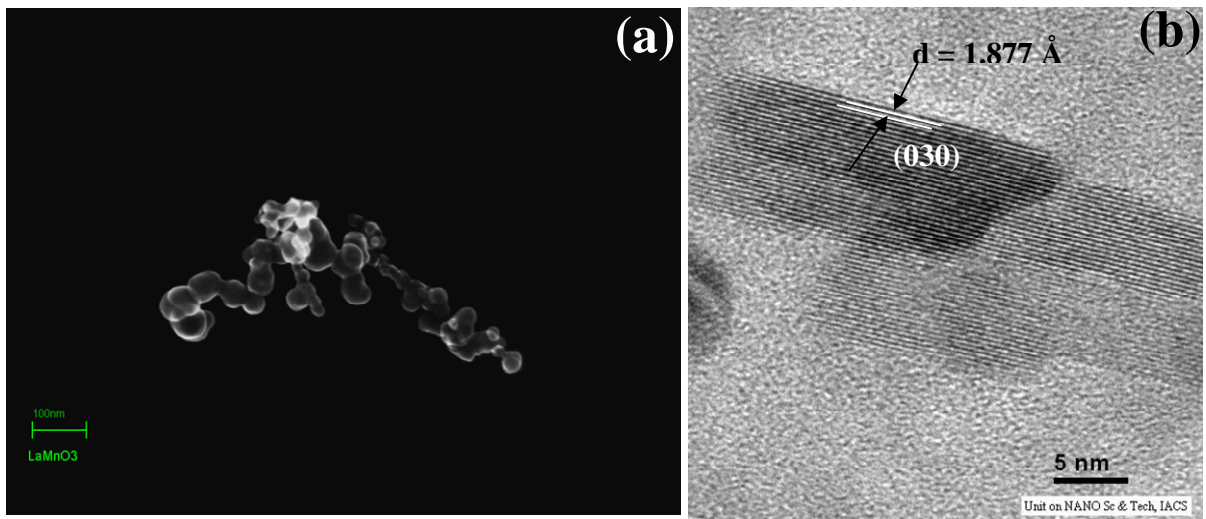


Fig.2. (a) The FESEM image of a nearly $\sim 1 \mu\text{m}$ long nanochain of LaMnO_3 whose diameters are $\leq 20 \text{ nm}$ at different places; (b) the high resolution transmission electron microscopy (HRTEM) image of the single crystalline nanorods of diameter 10-15 nm; (c) the room temperature x-ray diffraction pattern of LaMnO_3 (orthorhombic structure with $a = 5.443, b = 5.502, c = 7.707 \text{ \AA}$); little bit un-burnt carbon is also present.

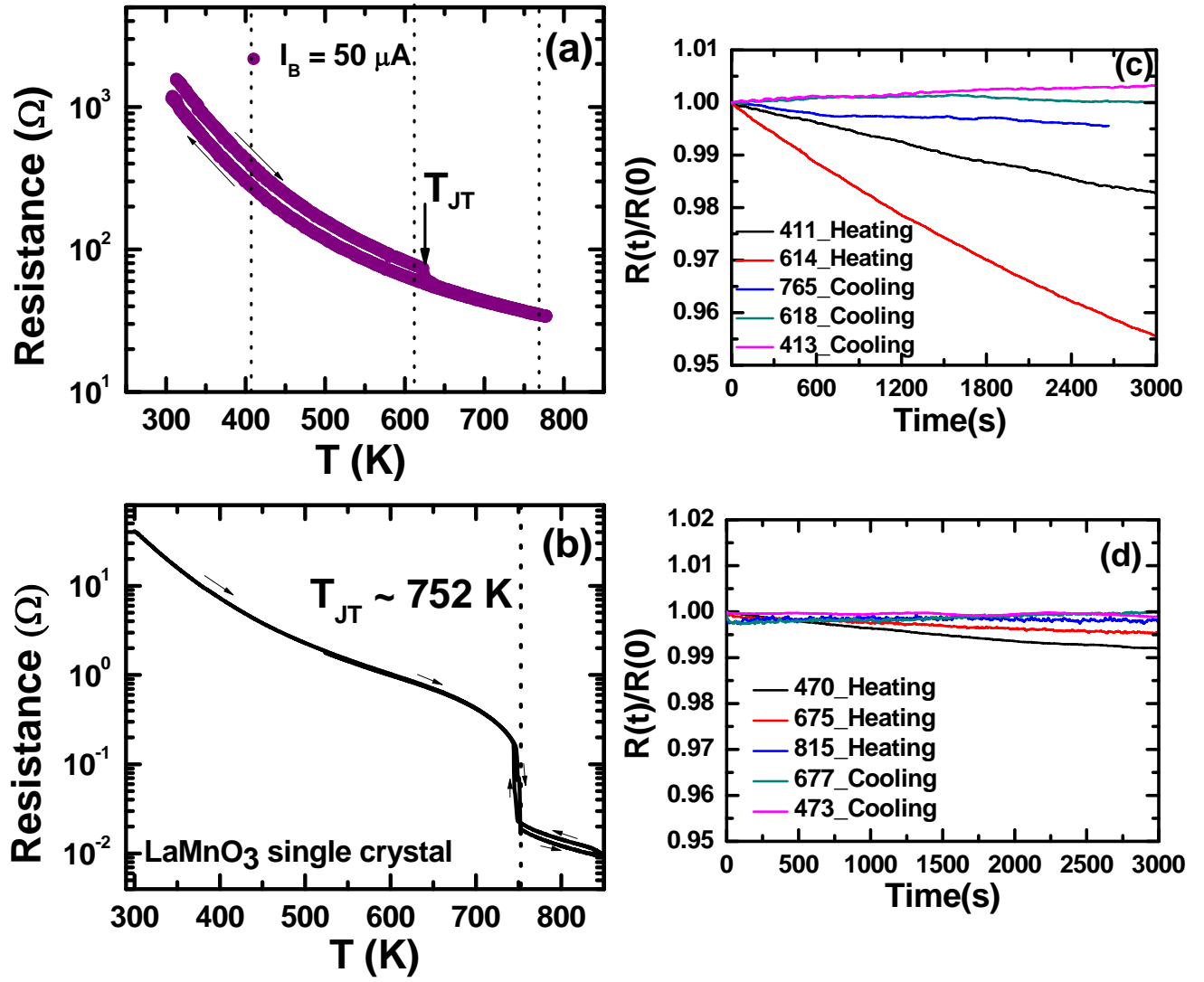


Fig.3. (color online) Resistivity versus temperature patterns for (a) nanoscale and (b) single crystal LaMnO₃; the time decay characteristics of the resistivity for (c) nanoscale and (d) single crystal LaMnO₃ in the orbital ordered and disordered phases reached via two different protocols.